



Deposited via The University of Leeds.

White Rose Research Online URL for this paper:

<https://eprints.whiterose.ac.uk/id/eprint/130666/>

Version: Accepted Version

---

**Article:**

Hussein, D, Collier, R, Lawrence, JA et al. (2017) Stratigraphic correlation and paleoenvironmental analysis of the hydrocarbon-bearing Early Miocene Euphrates and Jeribe formations in the Zagros folded-thrust belt. *Arabian Journal of Geosciences*, 10 (24). 543. ISSN: 1866-7511

<https://doi.org/10.1007/s12517-017-3342-0>

---

(c) Saudi Society for Geosciences 2017. This is a post-peer-review, pre-copyedit version of an article published in *Arabian Journal of Geosciences*. The final authenticated version is available online at: <https://doi.org/10.1007/s12517-017-3342-0>.

**Reuse**

Items deposited in White Rose Research Online are protected by copyright, with all rights reserved unless indicated otherwise. They may be downloaded and/or printed for private study, or other acts as permitted by national copyright laws. The publisher or other rights holders may allow further reproduction and re-use of the full text version. This is indicated by the licence information on the White Rose Research Online record for the item.

**Takedown**

If you consider content in White Rose Research Online to be in breach of UK law, please notify us by emailing [eprints@whiterose.ac.uk](mailto:eprints@whiterose.ac.uk) including the URL of the record and the reason for the withdrawal request.

# **Stratigraphic correlation and palaeo-environmental analysis of the hydrocarbon bearing Early Miocene Euphrates and Jeribe formations in the Zagros Folded-Thrust belt.**

**Hussein, D.<sup>1</sup>, Collier, R.<sup>3</sup>, Lawrence, J.A.<sup>2</sup>, Rashid, F.<sup>4</sup>; Glover, P.W.J.<sup>4</sup>, Lorinczi P.<sup>3</sup>, Baban, D. H.<sup>1</sup>**

<sup>1</sup> Geology Department, University of Suliamani, Kurdistan region, Iraq

<sup>2</sup> Department of Civil and Environmental Engineering, Faculty of Engineering, Imperial College, London, UK.

<sup>3</sup> School of Earth and Environment, University of Leeds, UK.

<sup>4</sup> Oil, Gas and Energy Management Department, Charmo University, Kurdistan region, Iraq.

## **Abstract**

The Lower Miocene Euphrates and Jeribe formations are considered as the main targets of the Tertiary petroleum system in the western part of the Zagros Basin. The formations consist of carbonates with some evaporate intercalations of the Dhiban Formation. This study utilized data from a field investigation including newly described outcrop sections, newly discovered productive oil fields within the Kirkuk embayment zone of the Zagros Fold and Thrust belt such as Sarqala and Kurdamir wells. This work is the first to show a stratigraphic correlation and palaeoenvironmental interpretation by investigating both well data and new outcrop data.

Three depositional environments were identified, an:

1. Inner and outer ramp belts environment;
2. shoal environment; and
3. restricted lagoon environment.

Within these three environments twelve microfacies were identified, based on the distribution of fauna mainly benthonic foraminifera, rock textures and sedimentary structures. The inferred shallow water depths and variable salinities in both the Euphrates Formation and Jeribe formation carbonates are consistent with deposition on the inner ramp (restricted lagoon and shoal) environments. Those found in the Euphrates Formation constrained the depositional environment to the restricted lagoon and shoal environment, whilst the microfacies in the Jeribe Formation provided evidence for an inner ramp and middle to outer ramp belt environments. This study represents the first detailed research that focuses on the stratigraphic correlation and changes in carbonate facies with the main aim to provide a wider understanding of stratigraphy of these carbonate reservoirs throughout the northern part of Iraq.

Keywords:

Carbonate ramp, Palaeoenvironments, Early Miocene carbonates, Zagros.

## 1. Introduction

The Zagros Folded and Thrust Belt (ZFTB) has one of the largest petroleum reserves in the Middle East, which is characterized by multiple petroleum systems with a wide range of producing and potential reservoirs (Aqrabi *et al.*, 2010; Jassim and Goff, 2006). Reservoir systems are commonly found within the Cretaceous and Tertiary, as well as in the Triassic and Jurassic, most of which are considered to have producible reserves. Many wells have been drilled recently in the Kurdistan region of Iraq, and a number of new fields have been discovered (Aqrabi *et al.*, 2010; Zebari and Burberry, 2015; Rashid *et al.*, 2017). These fields are generally elongated and follow a general NW-SE trend, consistent with the ZFTB structures (Zebari and Burberry, 2015; Awdal *et al.*, 2013; Rashid *et al.*, 2015a, b). Consequently, a clear understanding of the sedimentological and geological history of the region is fundamental to reservoir development.

In the Kurdistan region of Iraq the most targeted reservoirs occur in the Lower Miocene Euphrates and Jeribe formations which are folded into major structures (i.e., the Kormor, Sarqala and Kurdamir anticlines). Both formations are composed of inner shelf carbonates with a primary matrix porosity and a secondary porosity due to dolomitization (Aqrabi *et al.*, 2010; Jassim and Goff, 2006).

Early Miocene formations have been studied and recorded by several authors in many areas of Iraq, including the central and western parts (Al-Juboury *et al.*, 2007; Al-Juboury *et al.*, 2010). However, they have not been analyzed in detail from outcrop studies in the Kurdistan region of northern Iraq, the Lower Miocene Dhiban and Jeribe formations having been described previously from borehole studies (Al-Juboury *et al.*, 2007; Western Zagros Final well reports, 2011).

This study investigates the microfacies of the Lower Miocene Euphrates and Jeribe formations in the Kurdistan region, outlining the microfacies variation within five outcrop sections (Figure 1) and comparing these with core obtained from the more central and basinal locations to the west and south-west including the Kirkuk embayment. This study represents the first detailed research that focuses on the stratigraphic correlation and changes in carbonate facies with the main aim to provide a wider understanding of stratigraphy of these carbonate reservoirs throughout the northern part of Iraq.

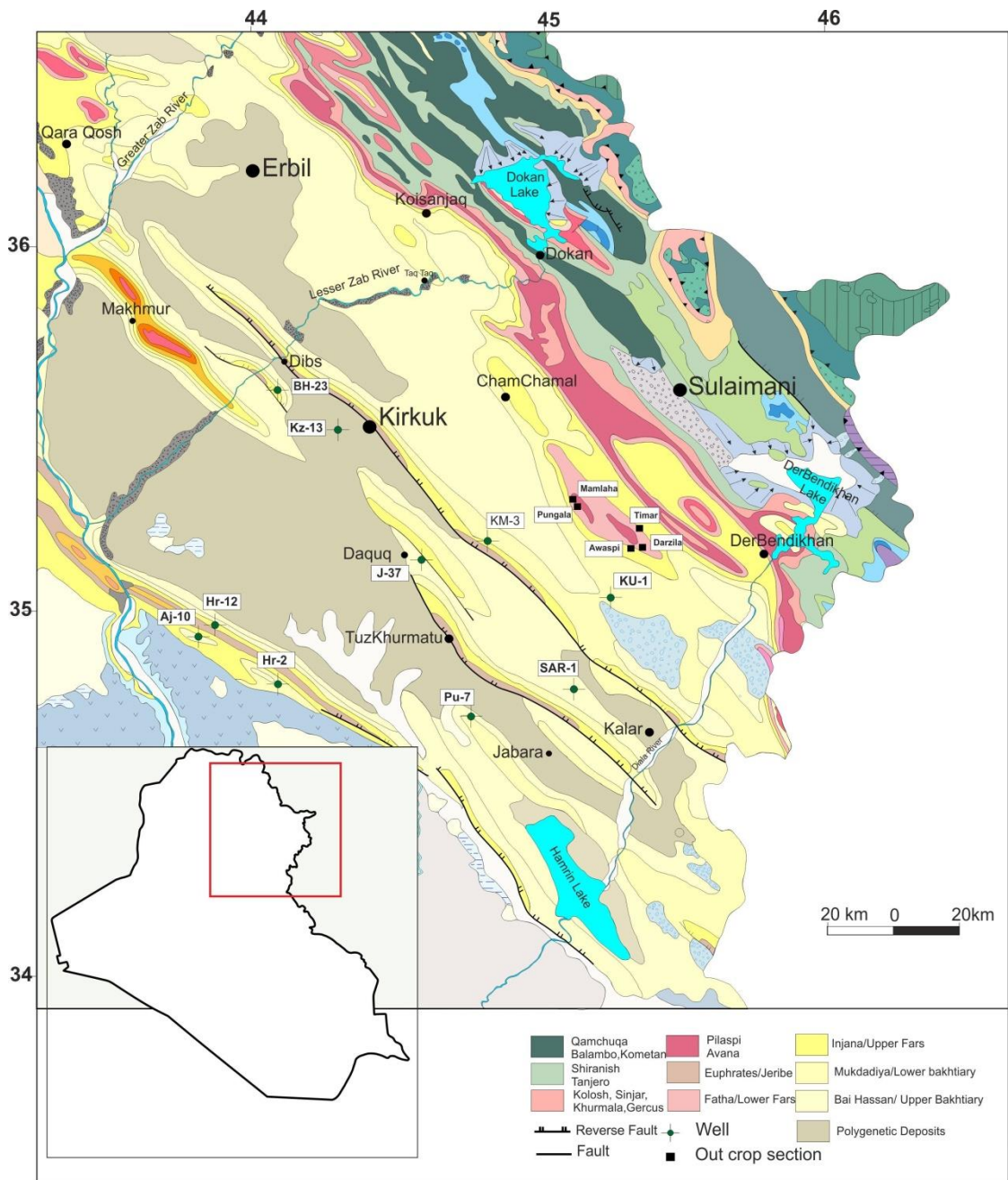


**Fig. 1** Geological map of Kurdistan region and north east of Iraq shows the selected fields, blocks and outcrop section of the study area, modified from (Sissakian et al., 2000).

### Geological setting

The study area is located in the Kurdistan region in the northern part of Iraq, and tectonically within the Low Folded Zone (LFZ) of the Iraqi main tectonic segments (Figure 1), which is characterized by the existence of NW-SE trending low amplitude folds separated by relatively wide synclines (Jassim and Goff, 2006).

The Euphrates Formation is of Aquitanian age (Figure 2). It is a shelly, chalky, well-bedded, recrystallized limestone, with occasional anhydrite in some subsurface sections, the latter which are possibly tongues of the Ghar or Dhiban formations. The Euphrates Formation consists mainly of limestones with textures ranging from oolitic to chalky, which locally contain corals and shell coquinas that are often recrystallized and siliceous. Beds of argillaceous sandstones, breccia's, conglomerates, and conglomeratic limestones also occur (Jassim and Goff, 2006). The largest measured thicknesses of the Euphrates Formation are 80 m and 90 m, occurring in the Hamrine and Ajeel oil fields, respectively. However, according to Bellen *et al.* (1959), the type locality of the Euphrates Formation is near Wadi Fuhaimi where it is only 8 m thick. The type location is clearly somewhat unrepresentative of the wider formation (Figure 3A).

In the area under study, the Euphrates Formation is underlain by conglomeratic layers and reefal limestone of the Oligocene Anah Formation (Figure 2). The reefal facies of the Anah Formation were only observed in one of the studied outcrops (Darzila section) together with palaeosol (Figure 4C). However, the basal conglomeritic layer was observed at the other four outcrops (Figure 4B). The Euphrates Formation is separated from the overlying younger Jeribe Formation by the Dhiban Formation (Figure 2 and Figure 3A). The Dhiban Formation consists of laminated to massive anhydrites with halite occurring locally at its base, and has a maximum thickness of 173 m (Al-Juboury *et al.*, 2007; Aqrabi *et al.*, 2010)

The Jeribe Formation is of Burdigalian age and consists of bedded (1-2 m thick beds) recrystallized and dolomitized limestones. The type locality of the Jeribe Formation is near Jaddala village, Jebel Sinjar, where it has a thickness of 73 m (Figure 3B). The Euphrates and Jeribe Formations can not be differentiated in the field when the intervening Dhiban Formation anhydrites are absent. (Figure 2). The red claystone of the Fat'ha Formation overlie the Jeribe Formation (Bellen *et al.*, 1959).

Grabowski and Liu (2010) propose a Lower Miocene age for the Jeribe and Euphrates formations based on strontium isotope measurements. These measurements indicate the oldest rocks are the Serikagni and Euphrates Formations from the late Chattian to early Aquitanian (24.3-21.8 Ma). The platform carbonates of the Jeribe Formation are early to middle Burdigalian in age (19.6-18.5 Ma), and the evaporites of the Dhiban Formation were deposited from the late Aquitanian to early Burdigalian (21.3-19.6 Ma). Buday (1980), Jassim and Goff (2006) and Al-Juboury *et al.*(2007) had all previously indicated a Middle

Miocene age for the Jeribe Formation. Whilst [Aqrabi et al. \(2010\)](#) inferred that the Jeribe Formation was previously dated erroneously.

## 2. Methodology

The data used in this work was gathered from the Kurdistan region, which encompasses the Azhdagh and Mamlaha anticlines ([Figure 1](#)) in the Low Folded Zone. Five outcrop sections of the Jeribe Formation and the Euphrates Formation were selected at Darzila, Awaspi, Timar, Mamlaha and Pungala and well data was collected from 10 drilled wells in the, Kormor, Bai Hassan, Khbaz, Pulkhana, and Hamrine fields of the Low Folded Zone (see [Figure 1](#) for location).

A total of 518 core plug samples from the studied wells and outcrops samples together with wireline log data from 10 wells were analysed. The core plug samples were analysed by their grain size and type, colour and fossil content. The facies and microfacies of the limestone formations were studied and characterized through detailed sedimentary logging, petrographic analysis and XRD diffraction measurements, as well as identification of their sedimentological properties.

Thin sections were made from all of the rocks and core samples for examination using a polarizing microscope. Thin sections were stained by using three different solutions including hydrochloric acid (HCL), Alizarin Red S (ARS) and Potassium Ferricyanide (PF) based on [Dickson's \(1965, 1966\)](#) procedure.

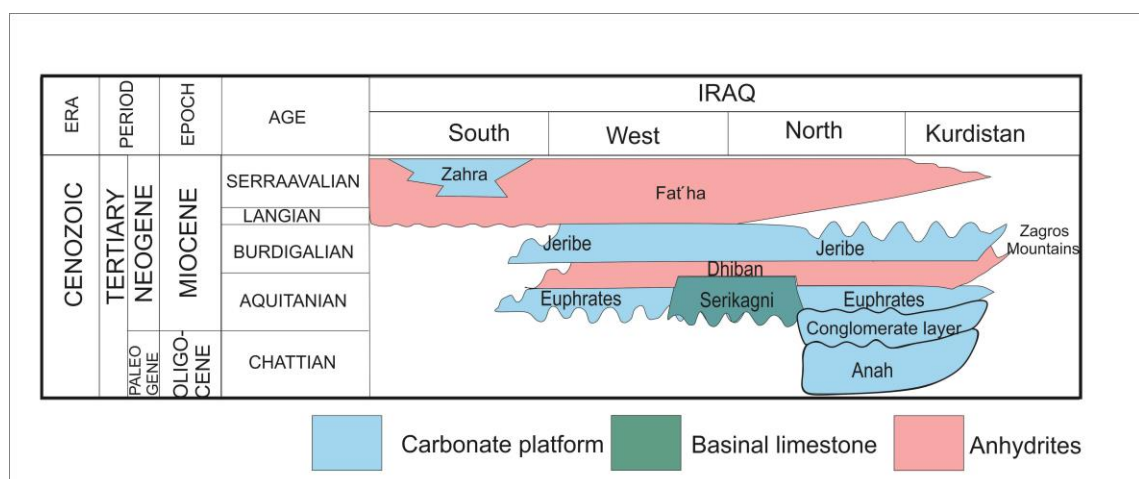


**Fig. 2** Chronostratigraphic chart of Iraq (after Petroleum Geo-service, 2000).

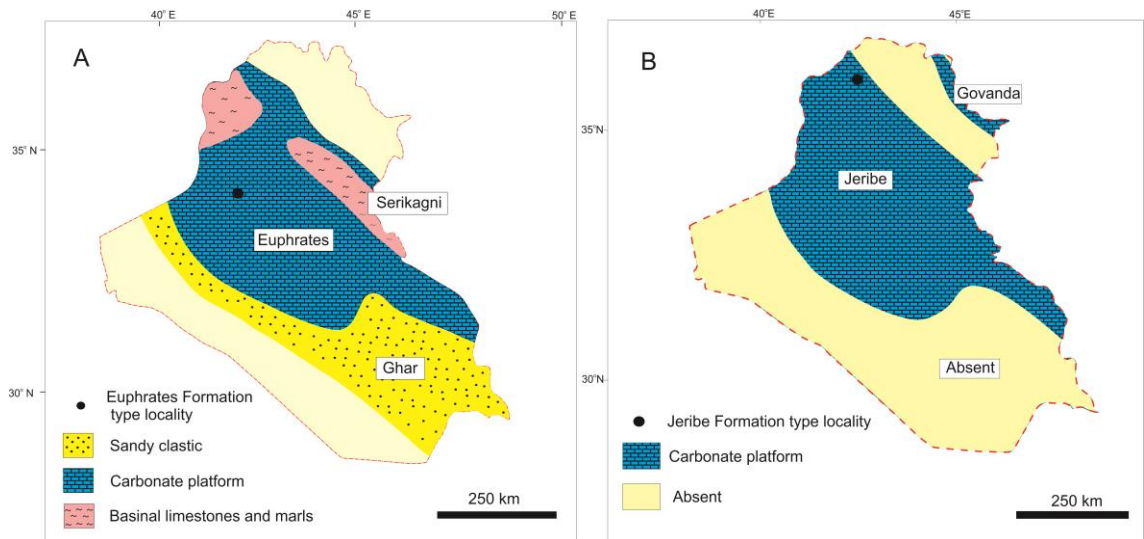


**Fig. 3 a** Latest Chattian-Early Aquitanian palaeogeography of Iraq, **b** Late Aquitanian- early Burdigalian palaeogeography of Iraq (after Aqrawi et al., 2010).

Detail of the most common components of carbonate rocks was based on Dunham (1962), Tucker and Wright *et al.* (1990), Geel (2000), Moore (2001), Nichols (2001) and Flugel (2004; 2010).

The available well data included a gamma ray log (GR), a bulk density log (RHOB) and a neutron porosity (NPHI) log. The gamma ray log was used to quantify the clay content of the rocks and the bulk density neutron logs combination were used to help determine lithology in un-cored intervals.

### 3. Results

#### 3.1. Stratigraphy

The Early Miocene Euphrates and Jeribe formations were observed throughout the outcrops. The lower contact of the Euphrates Formation is determined by a change from the underlying reefal limestone of the Oligocene Anah Formation (Figure 4A) that is sometimes interrupted by a conglomeritic layer and a palaeosol layer as shown in Figure 2. The upper contact of the Euphrates Formation is determined by the occurrence of the evaporites of the Dhiban Formation upon which the highly fractured and jointed limestone of the Jeribe Formation sits. The Jeribe Formation appeared in all sections as carbonates alternating with evaporitic carbonates. The upper contact of the Jeribe Formation is indicated by the claystone of the Fa'ha Formation of the Middle Miocene (Figure 5 and Figure 6).

#### **Conglomeritic and palaeosol layer:**

The Oligocene post-Anah limestone conglomerate formation consists of a 1 to 1.5 m thick unit of grey, poorly sorted, sub-angular to sub-rounded pebbles (4 mm to 64 mm in diameter), which extends laterally across all the studied outcrop sections. It contains reworked, recrystallized, fossiliferous limestone



**Fig. 4** a Field photograph of reeal limestone of the Oligocene Anah Formations in the Darzila sections, b Field photograph of the limestone conglomeratic beneath of the Euphrates Formation in the Awa Spi section, c Field photograph of the palaeosols layer in the Darzila section.

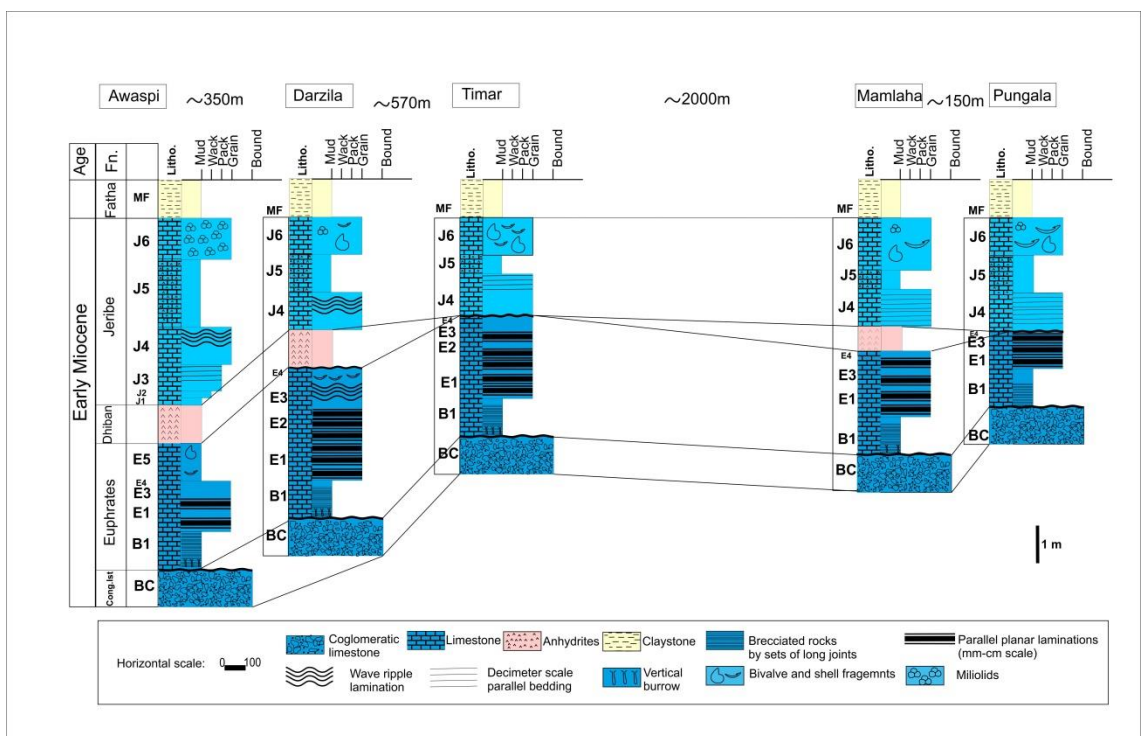


**Fig. 5** Stratigraphic sections of the Lower Miocene Formations along surface sections, showing thickness, lithological variations and the identified microfacies of the Euphrates Formation (E1, E2, E3, E4 and E5) also with the Jeribe microfacies (J1, J2, J3, J4, J5 and J6). Refer to Figure 1 for outcrop locations

pebble clasts of the underlying Oligocene formations. It has been interpreted by other authors (Buday, 1980; Sayyab and Abid, 1990; Al-Bakkal and Al-Ghreri, 1993; Al-Hammdani *et al.*, 2004) as a lower unit of the Euphrates Formation, while Al-Ghreri *et al.* (2010) has concluded that the conglomeritic layer dates back to the Late Oligocene-Early Miocene, because of the presence of clear reworked fossils, which relate it to reworking of the Anah Formation. The present study also interprets the alluvial origin of the conglomeritic layer as being derived from the underlying Oligocene formations (Figure 7A).

#### **Euphrates Formation:**

In outcrop, the marine Euphrates Formation sits above a flooding surface on top of the alluvial limestone conglomerate layer. The exposed surface sections of the unit include a basal “brecciated” layer, exemplified in the Darzila section (Figure 7B). This approximately 1 m thick basal carbonate shows an irregular mottled texture, especially in the upper part. The main part of the Euphrates Formation in outcrop is characterized by unaltered carbonate rock that overlies the brecciated unit. It appears in all sections with a thickness up to 4 m, with horizontal planar laminations in the lower part and the upper part characterized by grey-brownish laminated limestones with wave-generated sedimentary structures and a thin (ca. 200 mm) layer of dark grey limestone at the top. The penetrated thickness of the Euphrates Formation in the drilled wells available to this study ranges between approximately 30 m to >90 m. The Euphrates Formation can be recognized by the abrupt change in the density log (RHOB) and gamma ray log (GR) at the formation boundaries (Figure 6). White-grey dolomitic limestones with laminated sedimentary structures are observed in the collected core plugs from wells HR2 and KM3 (Table 2).

#### **Dhiban Formation:**

The Dhiban Formation is characterized at outcrop by a residual friable, yellow evaporitic layer, approximately 1 m thick, in boreholes the Dhiban Formation ranges from 5 m to 145 m thick. This unit is apparent at three exposed outcrop sections Awa Spi, Darzila and Mamlaha. In the subsurface it is recognized in all the studied drilled wells by high density and low gamma log readings for the evaporites, alternating with thin layers of dolomite and limestone.

#### **Jeribe Formation:**

The Jeribe Formation is 3-6 m in thickness at outcrop and consists of highly fractured, white, finely crystalline limestone

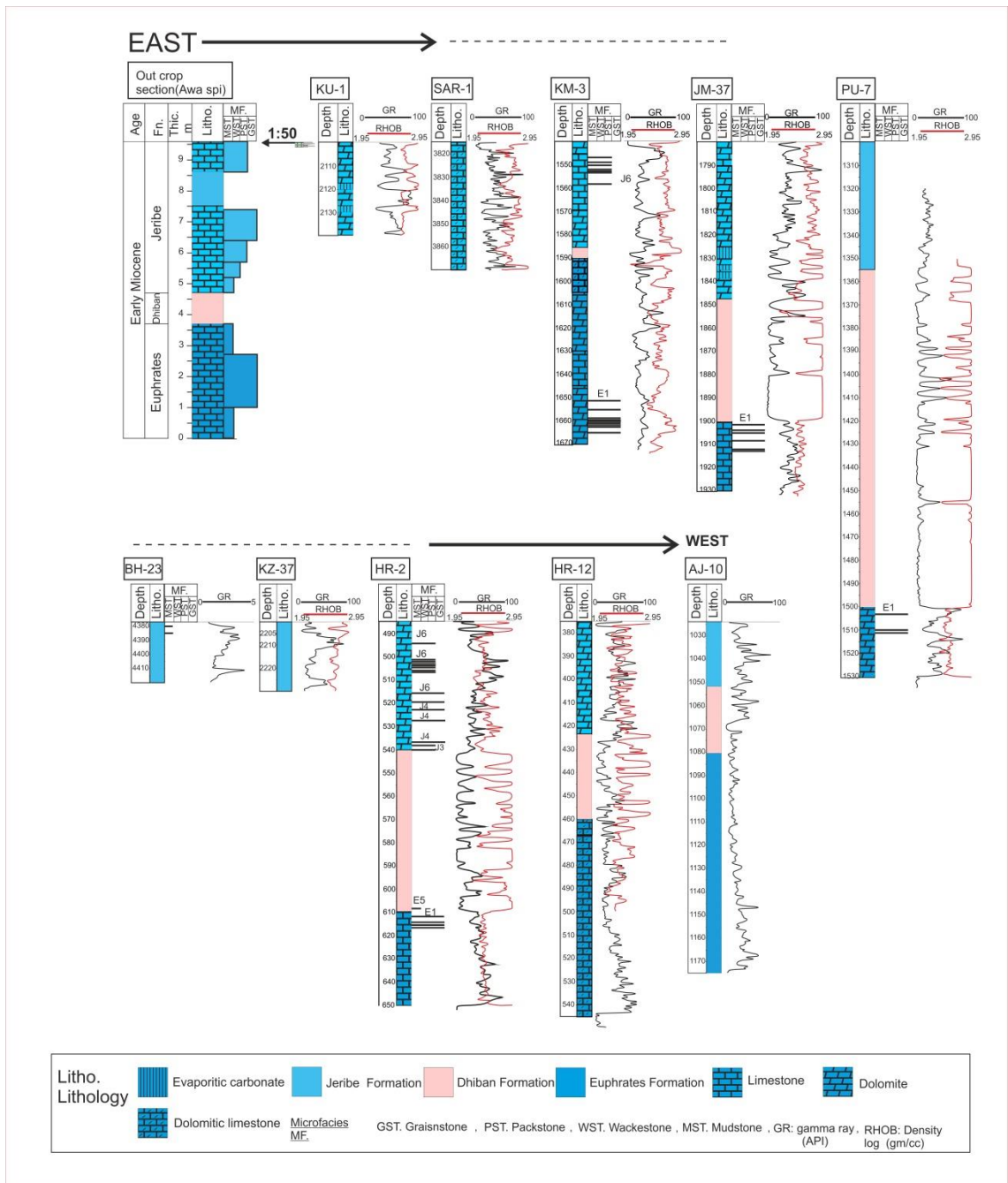


**Fig. 6** Stratigraphic sections of the Lower Miocene Formations along an approximately east to west transect, indicating gross lithological and thickness variations.

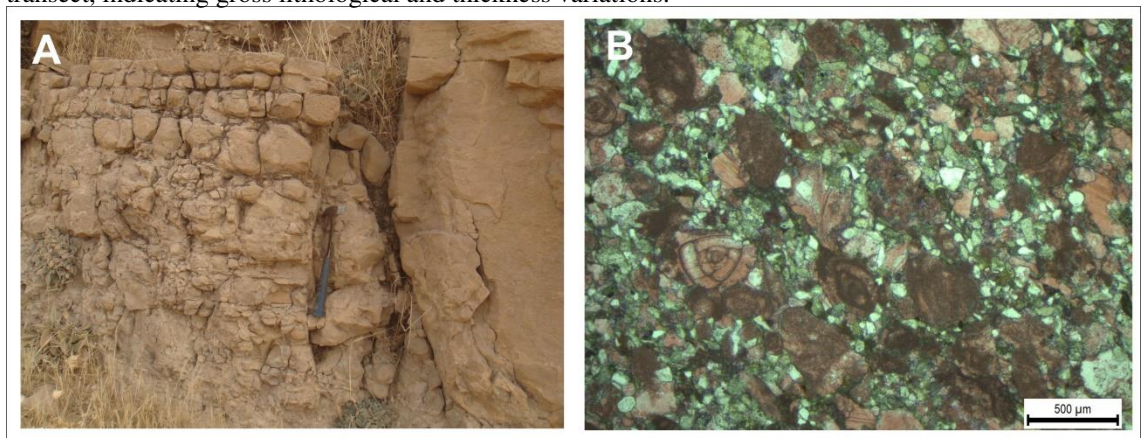


**Fig. 7 a** Field photograph of the “brecciated”, highly jointed basal layer of the Euphrates Formation from the Darzila outcrop section. **b** Photomicrograph of the “brecciate” basal unit of the Euphrates Formation:

a - reworked fossil from underlying beds, b - intraclast, c - angular quartz grain. Stained thin section from the Awa Spi outcrop section.

alternating with yellowish grey evaporitic carbonate. The lower contact of the Jeribe Formation is conformable with the underlying yellowish friable anhydrites of the Dhiban Formation and it is overlain by red claystone of the Middle Miocene Fatha Formation. The lower part of the Jeribe Formation is characterized by yellowish grey limestone and yellowish grey vuggy limestone, while shelly (fossiliferous) limestone is found in the upper part. A white-yellowish friable evaporitic carbonate (Figure 8) occurs in all outcrop sections, alternating with the limestone units.

Based on wireline logs (Figure 6) the subsurface Jeribe Formation in the study area consists of limestone and dolomitic limestone interbedded with anhydrites. The drilled thickness of the Jeribe Formation in the studied wells ranges between 20 m to > 65 m. The anhydritic layers are apparent in the JM37 and KU1 wells, whilst dolomite or dolomitic limestone is found in those other studied wells which show no anhydritic layer. The anhydritic interbeds of the Jeribe Formation are clearly shown by the combination of gamma ray logs and formation bulk density logs.

### 3.2. Microfacies analysis

Twelve different microfacies have been identified in the studied Euphrates Formation (microfacies B1, E1, E2, E3, E4 and E5) and Jeribe Formation (microfacies J1, J2, J3, J4, J5 and J6). They have been described based on fossil content, lithology and sedimentary structures. Five types of grainstone microfacies (B1 and E1 to E4) compose the majority of the Euphrates Formation, while mudstone microfacies (E5) dominate at its upper part. In the Jeribe Formation mudstone to packstone microfacies dominate (J1 to J6). The microfacies descriptions are given below and summarized in Table 3 and Table 4.

**Table 1** Geographic locations and samples types at studied surface sections.

Surface section	Formation	Total thickness (m)	Number of samples
Darzila	Jeribe	3	6
	Euphrates	4	5
Awa Spi	Jeribe	4.5	10
	Euphrates	3.7	8
Timar	Jeribe	3.2	6
	Euphrates	3.1	3
Mamlaha	Jeribe	2.9	5
	Euphrates	3	6
Pungala	Jeribe	3.2	4
	Euphrates	2.1	3

**Table 2** Geographic locations and well data at studied wells.

Drilled Well	Formation	Total Thickness (m)	Number of samples
Sarqala-1	Jeribe	51	-
Kurdamir-1	Jeribe	30	-
Kormor-3	Jeribe	45	6
	Euphrates	76	3
Hamrine-2	Jeribe	52	16
	Euphrates	42.2	5
Hamrine-12	Jeribe	46	-
	Euphrates	83	-
Ajeel-10	Jeribe	27.5	-
	Euphrates	92	-
Pulkhana-7	Jeribe	67	-
	Euphrates	30	3
Jambour-37	Jeribe	67	-
	Euphrates	31	6
Khabaz-37	Jeribe	21	-
Bai Hassan-23	Jeribe	20	2

### **Lithic-bioclastic grainstone (B1)**

This facies corresponds to the brecciated carbonate of the Euphrates Formation that forms a basal layer about 1 m thick in the field and is characterized by grey-greenish to brownish, parallel-bedded friable limestones. Its structure is highly jointed with bedding-perpendicular fractures spaced at typically 50-200 mm in the upper part. Bedding surfaces have also opened as joints. The brown colouration is more intense immediately adjacent (within 5 mm) of joint surfaces.

Vertical and horizontal burrows, *Skolithos* and *Planolites* respectively, occur within these carbonate grainstones. The “brecciated” material is composed of sand-sized reworked skeletal grains and lithoclasts derived from the underlying limestone conglomerate layer, which float in a silt-sized matrix (Figures 7B and 9A).



**Fig. 8** Field photograph of the evaporitic carbonate of the Jeribe Formation from Mamlaha section.

The nature of the lithoclasts and the angular, poorly sorted quartz grains from basin margin together with *Skolithos* and *Planolites* bioturbation indicate a short sediment transport residence time in a shallow marine environment of deposition, but with no wave-generated sedimentary bed forms apparent.

The “brecciated” unit of the Euphrates Formation may be related by diagenetic brecciation. Alternatively, Flugel (2010) for example, refers to pseudo-breccia’s in which there are in-place clasts which are separated by a network of joints, perhaps as a result of an earthquake.

#### **Bioclastic-Miliolid grainstone (E1)**

This microfacies is characterized grey bedded, unaltered limestone. The E1 microfacies overlies the brecciated limestone. It appears in all sections, with a total thickness of about 1 m. It is recognized in well Hamrine 2 at depths between 612 m and 614.3 m, and 615 m and 616 m, as well as in the Pulkhana, Jambour-37 and Kor Mor-3 wells. This facies contains horizontal planar (lamination) sedimentary structures. It has a skeletal grain-supported texture composed of different types of skeletal grains, including shell fragments (molluscs) and dominant imperforate and perforate benthonic foraminifera such as miliolids, rotaliids, and pelecypoda and gastropods together with medium-sized sand, ellipsoidal pellets and round to ellipsoidal ooids (Figure 9B).

The abundance of predominantly miliolid and rotaliids in this microfacies indicates a restricted, very shallow marine environment; rotaliids live in very shallow, turbulent water (Geel, 2000; Flugel 2010). In addition, grainstone texture and presence of parallel lamination indicate a relatively moderate to high energy level, influenced by waves and currents. The overall component of the bioclastic–miliolids microfacies indicates shallow marine environment above fair–weather wave-base.

### **Peloidal Grainstone (E2)**

The peloidal grainstone microfacies (E2) is characterized in the field by brownish-grey limestone. It occurs in the Darzila and Timar outcrop sections, but has not been found in the studied subsurface samples. In the Darzila section these grainstones have a total thickness of about 1 m, whilst in the Timar section they have 0.7 m.

This microfacies consists of peloidal grainstone that is composed of fine to very fine sand size, ellipsoidally- shaped pellets, and very fine sand-sized, sub-rounded ooids. Ooid nuclei are filled with ferroan calcite cement (Figure 9C). The main components of this microfacies are pellets, which are an indication that the depositional environment was a very shallow water setting, such as a lagoon (Tucker *et al.*, 1990). However, it is possible that they represent micritized foraminifera, in which case they would not indicate a specific water depth (Flugel, 2010). The absence of wave-generated structures indicates a low energy setting, again consistent with a lagoonal environment. Restricted conditions are suggested by rare to absent normal marine biota and abundant restricted biota (Geel, 2000).

### **Oolitic grainstone (E3)**

This microfacies is characterized in the field by grey-brownish laminated limestone that appears in all outcrop sections, with beds of only 0.1, 0.35 and 0.5 m thick, and a total thickness at the Darzila section of less than 1 m. The E3 microfacies has not been recognized in well samples. In outcrop obvious sedimentary structures are present in the form of wave ripple cross-lamination and planar cross-bedding.

The main grains of this microfacies are fine sand-sized, round and ellipsoidal ooids with a micritic structure and a minor component of very fine peloids (Figure 9D). The ooid nuclei include a few angular quartz grains or are replaced by ferroan calcite and the mineral glauconite. Bioclasts are also present, including benthonic foraminifera in the form of *Dendritina sp.*, peneroplids and gastropods. Grainstone texture and dominance of ooids indicates that the E3 microfacies indicate a high energy environment under the effect of waves and currents (Flugel, 2010). In addition, the wave ripple cross-lamination and

**Table. 3** Summary of microfacies, their main components and interpreted depositional environments for the Euphrates Formation. Gst. (grainstone), Pst. (packstone), Wst. (wackestone), Mst. (mudstone).

Microfacies	Microfacies Components	Sedimentary structures	Depositional environment
Lithic-bioclastic Gst. (B1)	Reworked skeletal grain& lithoclast from the underlying conglomeratic layer	Horizontal burrowing	Low-energy, very shallow environment, not affected by current and waves.
Bioclastic-Miliolids Gst. (E1)	Miliolids, rotaliids, pelecypoda and gastropod. Pellet and Ooids as secondary component.	Horizontal planar lamination	Restricted shallow marine environment, lagoonal to back-shoal.
Peloidal Gst. (E2)	Very fine to fine pellets with sub-rounded ooids	-	Mainly restricted lagoon.
Oolitic Gst. (E3)	Fine, rounded to ellipsoidal ooids and very fine peloids	Wave ripple cross lamination	shallow environment under the effect of waves and current activity- shoal barrier
Bioclastic ooidal Gst. (E4)	Fine to medium sand size, sub-rounded ooids, elongate peloid and shell fragments.	-	Shallow water, restricted lagoon towards back-shoal.
Mudstone (E5)	Calcareous mudstone, lime mud	-	Restricted lagoon.

**Table. 4** Summary of microfacies, their main components and interpreted depositional environments of the Jeribe Formation. Gst. (grainstone), Pst. (packstone), Wst. (wackestone), Mst. (mudstone).

Microfacies name	Microfacies components	Sedimentary structures	Depositional environment
Quartz-Mst. (J1)	Micritic lime, contain fine to very fine silt size angular quartz grain	-	Low energy, shallow water, lagoon or outer to middle ramp.
Quartz-Wst. (J2)	Lime mud, silt size quartz grain and cemented moulds of skeletal grain	-	Low energy environment, lagoonal or middle ramp.
Bioclastic-Pst. (J3)	Pelecypoda, gastropod and benthonic foraminifera.	-	Shallow water, inner ramp, normal marine salinities.
Gastropod-Gst. (J4)	Gastropod, pelecypod and bryzoa	Wave ripple cross lamination	Shallow water, shoal, variable salinity.
Restricted evaporitic carbonate (J5)	Recrystallized calcite matrix	-	Restricted hyper-saline, lagoon.
Miliolids-Pst. (J6)	Miliolids, rotaliids and shell fragment.		Very shallow, restricted lagoon.

planar cross-bedded sedimentary structures infer high energy wave activity or possibly tidal currents. Hence, the main characteristics of this facies indicate a very shallow marine environment, but of higher energy than that of the peloidal grainstone microfacies (E1 and E2).

#### **Bioclastic ooidal grainstone (E4)**

This microfacies is widely recognizable in the field as a thin layer of dark grey limestone. It occurs in all five outcrop sections within the study area, but does not appear in the studied samples from the drilled wells. It has a total thickness of approximately of only 0.1-0.2 m, but always occurs as the uppermost part of the Euphrates Formation, overlain by the friable yellowish-grey evaporite material of the Dhiban Formation.

This microfacies is characterized by a high abundance of fine to medium sand size sub-rounded, ellipsoidal ooids with a cortex which can be described as normal and superficial ooids. There with fine sand-sized, elongated peloids and shell fragments including bivalves and molluscs, and benthonic foraminifera in the form of miliolids and rotaliids (Figure 9E). There are small quantities of angular quartz grains. Characteristically, grains are commonly surrounded by a dark brown to yellowish microbial crust or envelope. Black bioclasts are also evident, particularly in the Mamlaha outcrop section, comprising thalli of coralline red algae (rhodolith fragments) which have previously been illustrated in Plate 8.16 of [Aqrawi \*et al.\* \(2010\)](#).

The nature of the grains and the abundance of the microbial encrusting in this microfacies indicate a shallow water environment ([Buxton and Pedley, 1989](#)). Furthermore, the interpretation of shallow water depth is supported by the occurrence of miliolids, which live in a variety of shallow water environments ([Geel, 2000](#)). The ooid structure of this microfacies indicates deposition in a moderate energy regime where there is some reworking by waves and currents. However, the variety of grain shapes and sizes implies a lower energy environment than that of the bioclastic-miliolid grainstone microfacies (E1) or the oolitic grainstone microfacies (E3).

#### **Mudstone (E5)**

This microfacies is characterized in the field by grey calcareous mudstone. It is only recognized in the Awa Spi section, where the total thickness of this mudstone microfacies is 1 m. In the subsurface it has been identified only in well Hamrine 2, at depths of 607 m to 608 m. It contains macroscopic bivalve

fossils such as pelecypoda. This microfacies consists of a micrite matrix (lime mud) with no foraminifera and only rare macro-skeletal grains (Figure 9F) and with very fine to fine angular grains of quartz. The characteristic feature of this mudstone microfacies is that it contains little or no fauna, which indicates that this facies was deposited in a protected lagoon (Flügel, 2004). The absence of fauna implies either hypersalinity or possibly the presence of clay in the water column, either of which could have inhibited colonization.

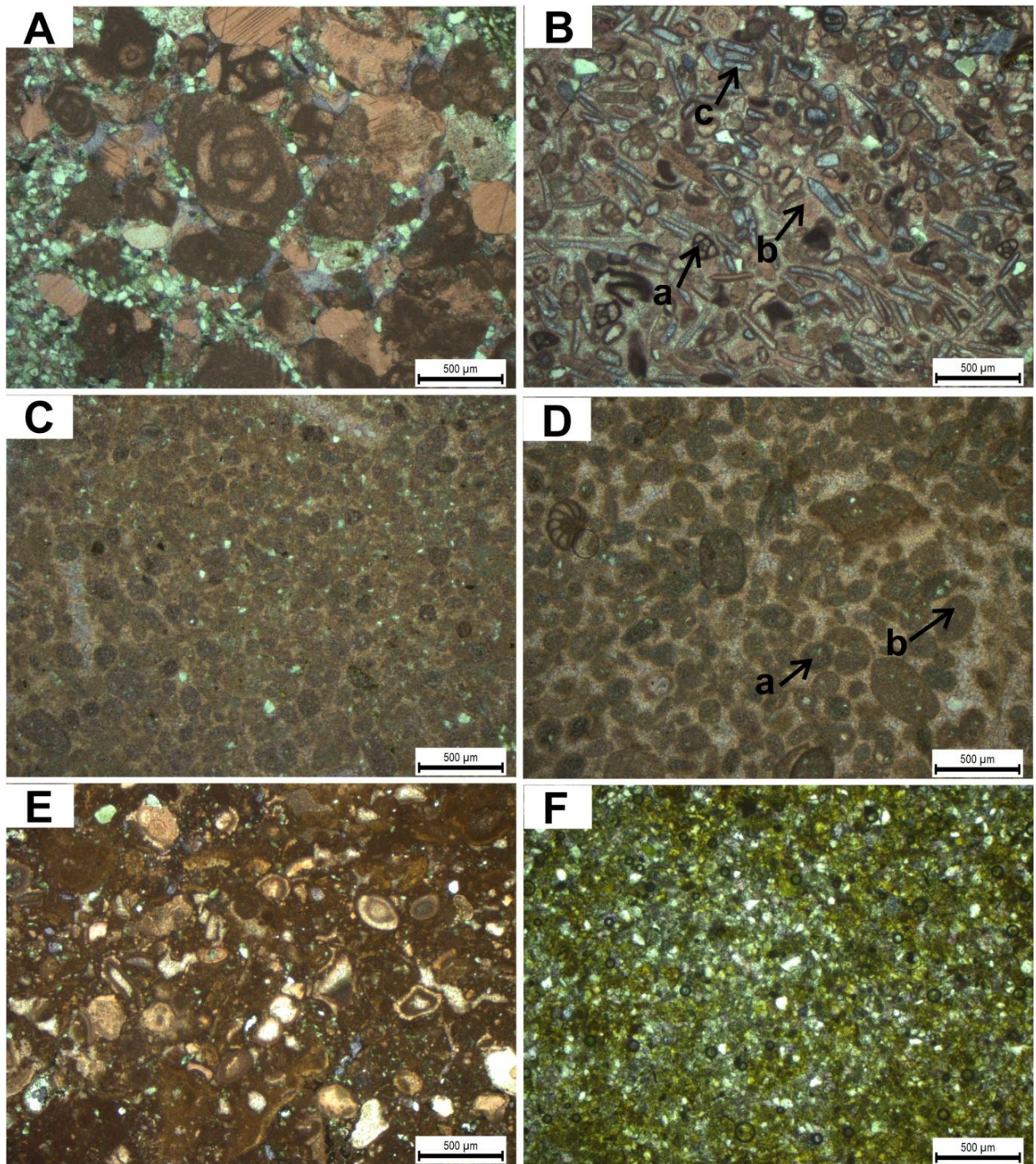


**Fig. 9 a** Photomicrograph of the brecciated grainstone B1 microfacies. Stained thin section from the Darzila outcrop section.

**b** Photomicrograph of the bioclastic-Miliolid grainstone microfacies E1: a - miliolids, b - shell fragment, c - Rotaliids. Stained thin section from the Awa Spi outcrop section, stained thin section from the Darzila section.

**c** Photomicrograph of the peloidal grainstone microfacies E2: a - ooids filled by ferroan calcite cement (arrowed) in a stained thin section from the Mamlaha outcrop section.

**d** Photomicrograph of ooidal grainstone microfacies E3: a - rounded ooids, b - ellipsoid ooid. Stained thin section from the Awa Spi outcrop section.

**e** Photomicrograph of the bioclastic ooidal grainstone microfacies E4.

**f** Photomicrograph of the mudstone microfacies E5, mainly composed of lime mud. Stained thin section from the Awa Spi outcrop section.

### **Quartz-mudstone (J1)**

This microfacies is characterized in the field by fine grey mudstones. Of the studied outcrops, it appears only in the Awa Spi section, with an average thickness of 0.5 m. It is recognized in the subsurface in well BH-23 at depths of 4370 ft and 4380 ft.

In outcrop it commonly overlies the evaporites of the Dhiban Formation and mainly consists of a micritic lime matrix, but also contains fine to very fine silt-sized detrital angular quartz grains, and low proportion of bioclasts. The bioclasts are identified as dendritinids and peneroplids (Figure 10A). This is consistent with a microfacies belonging to carbonate middle to outer ramp.

### **Quartz-wackestone (J2)**

This microfacies is characterized in the field by yellowish-grey limestone. It is recognized only in (the Awa Spi section), with a total thickness of 0.5 m. This microfacies consists of fine-grained quartz wackestone.

It is composed mainly of lime mud with of angular, fine silt-sized quartz grains, and more than 10% of cemented moulds of unidentified skeletal grains (Figure 10B). The nature of the matrix and the abundance of detrital quartz grains indicate that this microfacies was in a sub-wave base environment with raised salinities inhibiting faunal diversity. In the case of the Awa Spi section Facies J2 this is consistent with an accumulation in a middle ramp setting.

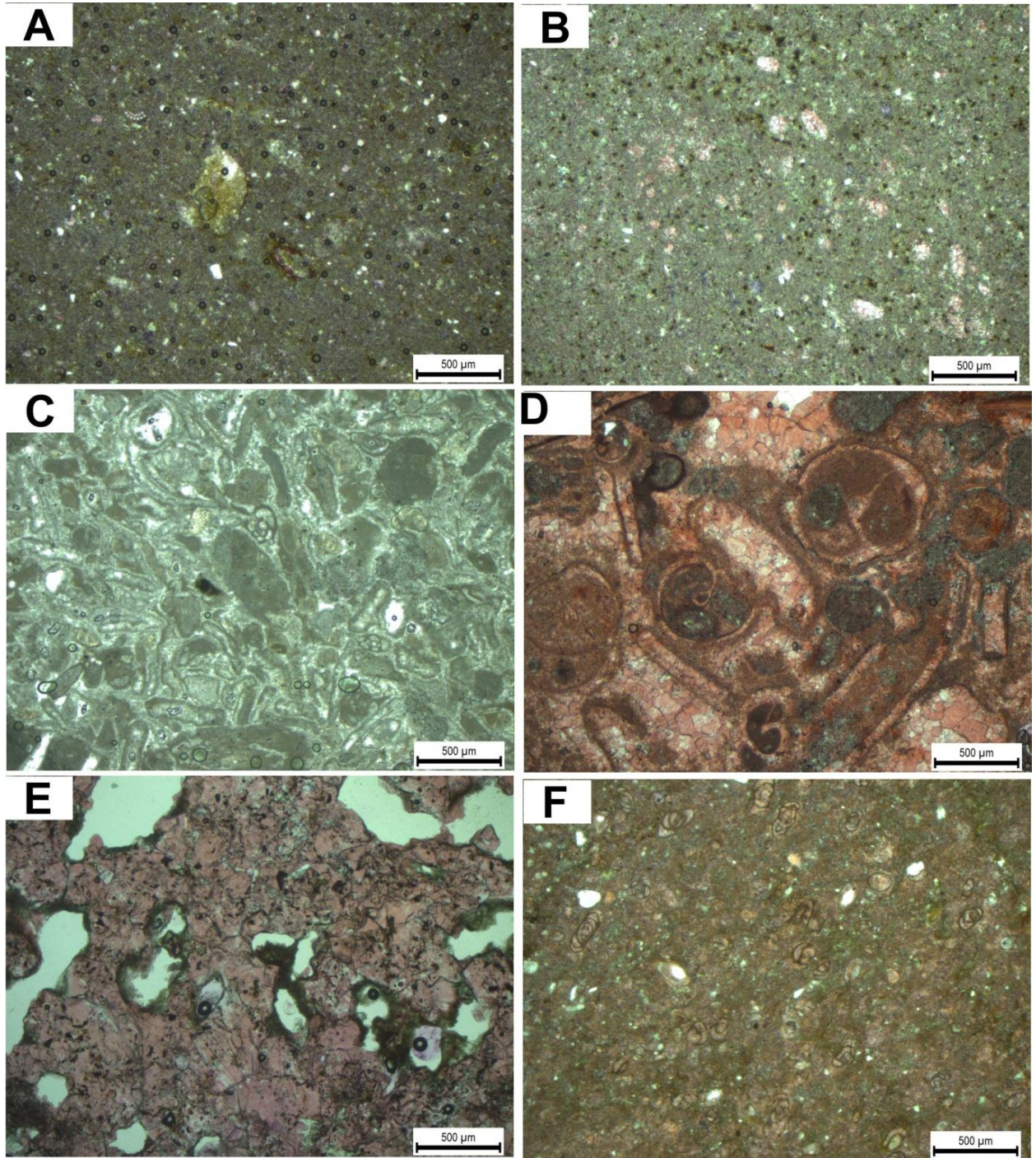


**Fig. 10 a** Photomicrograph of the quartz-mudstone microfacies J1, with silt size angular quartz grains.

**b** Photomicrograph of quartz-wackestone microfacies J2, with cemented molds after bioclastic grains. Stained thin section from the Awa Spi outcrop section.

**c** Photomicrograph of bioclastic-packstone microfacies J3. Stained thin section from the well HR2.

**d** Photomicrograph of gastropod-grainstone microfacies J4. Stained thin section from the Darzila outcrop section.

**e** Photomicrograph of the evaporitic-carbonate microfacies J5. Stained thin section from the Mamlaha outcrop section.

**f** Photomicrograph of the miliolids-packstone microfacies J6. Stained thin section from the Darzila section.

### **Bioclastic – packstone (J3)**

This microfacies appears in the field as white-yellowish limestone. It occurs in only the Awa Spi outcrop section, where it has an average thickness of approximately 0.7 m and is overlain by vuggy, shelly limestone. It is recognized in the Hamrine-2 well at depths of 539 m, 538 m and 540 m.

The main components of this microfacies are highly crystallized and micritized pelecypod, gastropods and benthonic foraminifera (Figure 10C). Bivalve fragments can be recognized by the outer shape or layer of the shells, which are cemented by granular mosaic cement. The bioclastic elements of subsurface samples consist of miliolids, shell fragments and brachiopods as well as echinoids and non-skeletal grains (peloid) which appear at a depth of 539 m. At this depth the microfacies is an echinoid-peloidal packstone. The identification of shell fragments of pelecypoda and elements such as echinoids suggest a shallow but normal marine salinity setting (Geel, 2000 and Flugel, 2010). Moreover, grains of this microfacies are highly micritized which is indicative of shallow marine environments in inner to middle ramp settings.

### **Gastropod-grainstone (J4)**

This microfacies is recognized in the field by a yellowish-grey vuggy, shelly (fossiliferous) limestone. It is identified in all outcrop sections with a total thickness of 1 m and is characterized by wave ripple cross-lamination sedimentary structures. It appears in the Hamrine-2 well at depths of 523 m, 527 m and 537.5 m. Its main components are gastropods, pelecypoda and bryozoa. It is composed of a high percentage of bivalve fragments and a very low percentage of sub-rounded, fine sand-sized ooids, plus shell fragments including mollusca and benthonic foraminifera such as miliolids, *Dendritina sp.*, peneroplids, rotalia, and algae (Figure 10D). The abundant gastropods of this facies suggests shallow water deposition such as in inner ramp settings (Geel, 2000). The grainstone texture and the presence of wave ripple cross-lamination indicates a high energy regime above the fair weather wave base.

### **Evaporitic-carbonate (J5)**

The J5 microfacies is characterized in the field by white-yellowish friable evaporitic carbonate, probably residual material after dissolution of some evaporites that were once present. It occurs in all outcrop sections. In the Awa Spi section it has a total thickness of 1.2 m, whilst it is slightly less thick (about 1 m) in the other sections. Based on field observations and petrography, this microfacies comprises a blocky

calcite cement (Figure 10E) with no fauna in the carbonate matrix, which suggests a setting of a hypersaline or lagoonal environment for possibly a marginal sabkha environment.

#### **Miliolids- packstone (J6)**

This microfacies is characterized in the field by grey fossiliferous limestone. It occurs at the top of the Jeribe Formation and is overlain by claystone of the Middle Miocene Fat'ha Formation. It is recognized in all studied outcrop sections with an average thickness of approximately 1 m. It is also identified in the Hamrine-2 well at depths of 491 m to 519 m, and is widely identified in core samples from the Kormor-3 well, where it also occurs with less matrix and so is strictly a miliolid grainstone. The miliolid-packstone microfacies contains miliolids, rotaliids and shell fragments such as oysters, and includes angular silt-sized quartz grains (Figure 10F). The abundance of miliolids in this microfacies indicates a very shallow restricted lagoonal environment (Geel, 2000). Furthermore, a low energy environment is also suggested by the presence of only silt grade quartz.

### **4. Ramp models Euphrates and Jeribe Formations**

The microfacies analysis carried out in this paper suggests shallow marine environments, based on the distribution of fauna and benthonic foraminifera, rock textures and sedimentary structures. The inferred shallow water depths and variable salinities in both the Euphrates Formation and Jeribe Formation carbonates are consistent with an inner ramp depositional setting encompassing mainly restricted lagoon and shoal sub-environments (Figure 11). The interpretation of the microfacies for each zone of the proximal ramp setting are described in the following sections.

#### **1-Euphrates Formation**

In the Euphrates Formation, the E3 oolitic grainstone microfacies is typical of an open, shallow marine shoal environment. This microfacies represents the least restricted, highest energy depositional environment encountered in the outcrop sections of the unit. The E1 bioclastic-miliolid grainstone facies may also extend into the shoal belt, on the basis of the presence of wave ripples and trough cross-bedding.

The abundant miliolids would, however, imply reworking of material from more restricted areas behind the shoal. The high diversity of miliolids and rotaliids with a few peneroplids in the bioclastic-miliolid grainstone microfacies (E1) and peloidal grainstone microfacies (E2) are also characteristic of a restricted, lagoonal environment (Geel, 2000).

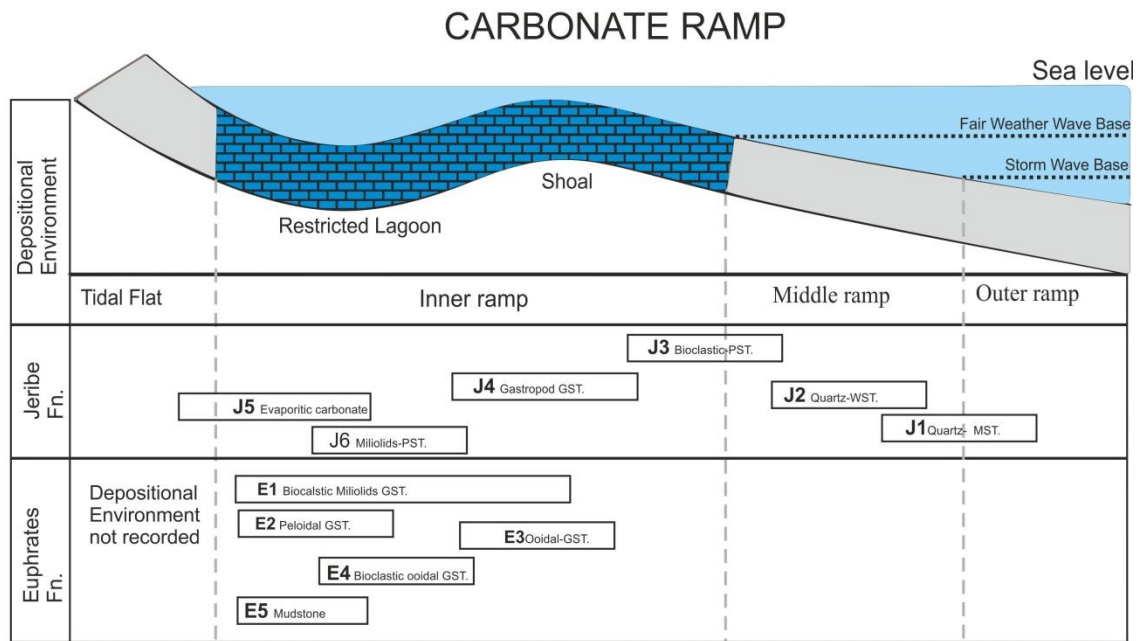


**Fig. 11** Depositional model for the Lower Miocene carbonate ramp of the Euphrates and Jeribe Formations in the Kurdistan region, NE Iraq.

The fine-grained character of the E5 mudstone microfacies and its absence of fauna apart from rare pelecypoda also indicate a relatively low energy environment with no evidence of wave and currents, hence its deposition in a restricted lagoon environment.

The encrusting of many of the bioclastic and ooidal grains in the bioclastic-ooidal grainstone microfacies (E4) indicates a relatively low energy part behind the shoal barrier, allowing time for the partial micritization of grains between reworking events. The high abundance of ooids grains, miliolids and rotaliids suggests reworking both from more restricted, hypersaline parts of the lagoon and from nearby higher energy, wave-reworked or shoal ooid-generating locations. The E4 microfacies is thus interpreted as representing an intermediate, facies between more restricted to more open and energetic facies, due to the abundance of miliolids and microbial encrusting with occurrence of variable sized ooids respectively

## 2-Jeribe Formation

The J1 quartz mudstone microfacies and the J2 quartz wackestone microfacies can each be interpreted as sub-fair-weather wave base, more distal facies of a carbonate ramp, however, given the restricted biota and lack of sedimentary structures in the Jeribe Formation quartz-mudstone microfacies (J1) and quartz-wackestone microfacies (J2) mean it is possible to interpret this as restricted lagoonal deposits (Geel 2000).

The J3 bioclastic-packstone microfacies of the Jeribe Formation may be interpreted as the most open marine element of the Jeribe Formation, given the presence of echinoids. The absence of wave-generated sedimentary structures suggests that it was deposited below the fair weather wave base. Therefore a middle ramp belt can be inferred, although a more open area behind any shoal/barrier or between shoal banks is also a possible interpretation of this microfacies in isolation. The J4 gastropod-grainstone microfacies is in the inner ramp belt (shoal belt), where fair-weather wave structures are not seen.

The bioclastic content of the J4 gastropod-grainstone microfacies indicates a very shallow marine environment, with gastropods and molluscs shells as the main components. The presence of wave ripples indicates it probably deposited in a high energy, very shallow marine shoal environment. The extent of wave and current activity in this environment will influence preservation of the shell and bivalve grains.

The evaporitic-carbonate microfacies (J5) and the miliolids-packstone microfacies (J6) are indicative of elevated salinities in a shallow, restricted water environment. The J5 microfacies represents, perhaps, the more marginal setting, towards a tidal flat margin. It is the abundance of miliolids in microfacies J6 which implies elevated salinities in a lagoonal setting (Flügel, 2010).

## 5. Discussion

### 5.1. Sedimentary trends and variations in ramp models for Euphrates and Jeribe Formations

Palaeoenvironmental interpretations of the five identified microfacies throughout the Euphrates Formation imply a single, overall regressive trend. An initial transgression is represented by the B1 brecciated grainstone over alluvial deposits of conglomeratic layer (Figure 4a). After this initial transgression in all outcrop sections, a regressive trend is recorded between low energy restricted lagoonal and shoal environments (E1, E2, E3, E4 and E5) which does not require any significant relative base level change and act to protect the restricted lagoon facies.

Six microfacies have been identified in the Jeribe Formation and interpreted for detailed depositional environments. The outcrop section at Awa Spi provides the most complete record of a single regressive, upwards hallowing cycle of deposition, based upon the sequence of microfacies from J1 to J6 (Figure 5). The interpretation of the lower part of the Jeribe Formation is carbonates of outer or middle ramp J1 quartz-mudstone microfacies pass up into the middle ramp J2 quartz-wackestone microfacies and then inner ramp J3 bioclastic-wackestone. Above this, J4 gastropod grainstones of the shoal belt occur, before passing up into J5 evaporitic carbonates and J6 miliolid packstones of the restricted lagoonal

environments landward of the advancing shoal belt. The other four outcrop sections appear to represent the upper part of the same regressive depositional cycle, but with microfacies J1 and J2 at the base being absent.

Sedimentological analysis of the Lower Miocene Formations at outcrop in the studied area indicates that the Euphrates and Jeribe formations were deposited in shallow-marine carbonate ramp environments. The identified microfacies were established in a middle to inner ramp belt, shoal and restricted lagoon environments of an overall relatively proximal ramp setting. Based on the variation in the main components and depositional textures of the described microfacies in outcrop exposures, ramp models are proposed for deposition of the Lower Miocene Euphrates and Jeribe formations (Figure 11). This implies that the initial transgression at the top of the Dhiban Formation reached greater water depths than the initial transgression recorded at the base of the Euphrates Formation at these outcrop locations. The single cycle of the Jeribe Formation that is exposed in outcrop is then characterized by an overall regressive trend, which overlapped the top of the Dhiban Formation from the Awa Spi location north-eastwards to the other four outcrop locations. The Euphrates Formation in outcrop represents an interplay between shoal belt microfacies, notably the E3 ooidal grainstones, and a restricted lagoon environment which is characterized by E1 bioclastic-miliolid grainstones and E2 peloidal grainstone microfacies, with the abundance of miliolids and peloids typically representative of this restricted environment. In addition, the nature of the E4 bioclastic ooidal grainstones and the E5 mudstone microfacies indicates deposition in more restricted, lower energy parts of the lagoon. The Jeribe Formation is distinct in its character from the Euphrates Formation, in including middle to inner ramp microfacies at its base. The J4 gastropod grainstones including pelecypod and shell fragment components indicate the existence of shoal environments in the Jeribe Formation. The J5 and J6 microfacies then indicate hypersaline conditions and at least elevated salinity episodes, respectively, in the lagoonal environments of the upper part of the observed regressive cycle.

## 5.2. Comparison with previous investigations

The depositional environment of the Jeribe Formation in central and southern Iraq has previously been described as a restricted to open platform, with sedimentation initially in a fore slope environment, passing up into lagoonal environments with variably open marine to restricted circulation ([-Juboury \*et al.\*, 2007](#); [Al-Juboury \*et al.\*, 2010](#)) or as a deep marine settings as suggested by [Al-Dabbas \*et al.\* \(2013\)](#). The sedimentary analysis presented in this work has shown a carbonate ramp model is most likely, based upon observations which correspond to standard elements of carbonate ramps such as a low angle slope, distal to proximal coarsening trends, and back-shoal variously restricted to open marine lagoonal environments (after [Burchette, and Wright 1992](#)). A comparable model has been described for the laterally equivalent Asmari Formation in the Dezful Embayment in SW Iran ([Aqrawi \*et al.\*, 2006](#)), which is the main petroleum reservoir in south-west Iran, and where production properties are based on the development of fracture networks ([Wennberg \*et al.\*, 2006](#)).

The Euphrates and Jeribe formations in the study area reveal differences in detailed microfacies, but broadly consistent facies trends overall, conforming to minor variations of the basic carbonate ramp model. What is also apparent is that the outcrops studied in the Kurdistan region represent the more proximal end of a carbonate ramp that extended more than 100 km to the south-west into the Zagros Basin (Figure 1). Only the J1 quartz mudstone and the J2 quartz wackestone microfacies represent outer ramp, sub-storm wave-base environments. Most of the microfacies present in both formations represent shoal to lagoonal facies in outcrop. In the wells to the south-west, however, log signatures indicate that more complete shallowing-upwards cycles are present ([Figure 6](#)), with clay-rich outer ramp facies indicated by higher gamma-ray counts in the lower part of each cycle. This confirms the overall palaeogeographic trend of a gradual north-east to south-west depositional gradient, with more and more complete depositional cycles being preserved toward the basin centre to the south-west. In addition tectonic activity in the Early Miocene caused sea fluctuations to generating regressions and transgressions ([Aqrawi \*et al.\*, 2010](#)), the deposits laid down during the regression form thin formations in the proximal area of the basin such as outcrop sections of the Early Miocene formations in the Kurdistan region. The transgressive deposits form a thick formation in more distal part of the basin as seen in the Euphrates successions in the Ajeel well (Final well report, NOC, 1997).

## 6. Conclusion

Tertiary carbonates are the main petroleum systems in the Zagros Basin. However very little is known about the palaeoenvironment and stratigraphic correlation of the Lower Miocene carbonate formations in the Kurdistan region, on the north-east margin of the Mesopotamian Basin. This integrated study used data from previously un-investigated outcrops and core samples, petrophysical log data and petrographical analysis of the rock samples. This work is the first to show a stratigraphic correlation and palaeoenvironmental interpretation of the Lower Miocene Euphrates and Jeribe formations investigating both well data and new outcrop data in this region.

Across the Euphrates and Jeribe formations twelve microfacies were identified. Analysis of these microfacies indicates shallow marine environments, based on texture, sedimentary structures and fauna (mainly foraminifera). The inferred shallow water depths and variable salinities in both the Euphrates Formation and Jeribe Formation carbonates are consistent with deposition on the inner part of a carbonate ramp. More specifically, the microfacies led to the interpretation of restricted lagoon and shoal palaeoenvironment in the Euphrates Formation and a restricted lagoon and shoal in an inner and middle ramp belt environment in the Jeribe Formation.

## Acknowledgments

This study was funded by the Ministry of Higher Education of the Iraqi Kurdistan region government as a part of the Human Capacity Development Programme (HCDP) that is greatly appreciated. We express our gratitude to the Ministry of Natural Resources of Kurdistan region for providing two licensed block data and the Ministry of Oil of the Iraqi government for providing well data.

## References

- Al-Bakkal, K. K., and M. F. Al-Ghreri, 1993, Sedimentological and paleontological study of Oligocene-Miocene boundary basal conglomerate unit, Western Iraq: *J Sci*, v. 2, p. 22-27.
- Al-Ghreri, M. F., A. S. Sayyab, and J. A. Jassim, 2010, Remarks on the age of the Miocene Euphrates Formation, Western Iraq: *Fifth Scientific Environmental Conference, Zagazig university, Egypt*, p. 185-195.
- Al-Hammdani, A. M., S. Q. Al-Naqib, and K. T. Al-Youzbaki, 2004, Facies Analysis and depositional environments of the Euphrates Formation between Fuhaimi and Al-qaim valleys, in western desert-Iraq. *Raf. J. Sci*, v. 16, p. 45-55.

- Al-Juboury, A. I., J. S. Al-Ghrear, and M. A. Al-Rubaii, 2010, Petrography and diagenetic characteristics of the Upper Oligocene – Lower Miocene Ghar Formation in SE Iraq. *Journal of Petroleum Geology*, v. 33, p. 67-85.
- Al-Juboury, A., A. Al-Tarif, and M. Al-Esa, 2007, Basin analysis of the Burdigalian and Early Langhian successions, Kirkuk basin, Iraq: Geological society, London, Special publication, v. 258, p. 53-68.
- Aqrawi, A. A. M., J. C. Goff, A. D. Horbury, and F. N. Saddni, 2010, *The petroleum geology of Iraq*: Scientific Press Ltd, Beacon field, Bucks.
- Aqrawi, A. A. M., M. Keramati, S. N. Ehrenberg, N. Pickard, A. Moallemi, T. Svånå, G. Darke, J. A. D. Dickson, and N. H. Oxtoby, 2006, The origin of dolomite in the Asmari Formation (Oligocene-Lower Miocene), Dezful Embayment, SW Iran. *Journal of Petroleum Geology*, v. 29, p. 381-402.
- Awdal, A. H., A. Braathen, O. P. Wennberg, and G. H. Sherwani, 2013, The characteristics of fracture networks in the Shiranish Formation of the Bina Bawi Anticline; comparison with the Taq Taq Field, Zagros, Kurdistan, NE Iraq. *Petroleum Geoscience*, v. 19, p. 139-155.
- Bellen, R. C. V., H. Dunnington, R. Wetzel, and D. Morton, 1959, *Lexique stratigraphique: International, Asie, Iraq*.
- Buday, T., 1980, regional Geology of Iraq, v. 1, Stratigraphy and paleogeography: DG of Geological Survey and Mineral Investigation.
- Burchette, T., and V. P. Wright, 1992, Carbonate ramp depositional systems: *Sedimentary Geology*, v. 79, p. 3-57.
- Buxton, M. W., and H. M. Pedley, 1989, A standardized model for Tethyan Tertiary carbonate ramps: *Journal of Geological Society*, v. 146, p. 746-748.
- Dickson, J. A. D., 1965, A modified staining technique for carbonates in thin section: *Nature*.
- Dickson, J. A. D., 1966, carbonate identification and genesis as revealed by staining: *Journal of sedimentary petrology*, v. 36, p. 491-505.
- Dunham, R. J., 1962, Classification of carbonate rocks according to depositional texture: *American Association of Petroleum Geologist Bulletin*, v. 1, p. 108-121.
- Flügel, E., 2004, *Microfacies of carbonate rocks: analysis, interpretation and application*: Springer Verlag, 984 p.
- Flügel, E., 2010, *Microfacies Of Carbonate Rocks*: Verlag Berlin Heidelberg, p. 984.

- Geel, T., 2000, Recognition of stratigraphic sequences in carbonate platform and slope deposits: empirical models based on microfacies analysis of Palaeogene deposits in southeastern Spain: *Palaeogeography, Palaeoclimatology, Palaeoecology*, v. 155, p. 211-238.
- Ghafur, A. A., 2012, Sedimentology and reservoir characteristics of the Oligocene-Early Miocene carbonates (Kirkuk Group), Cardiff University, 299 p.
- Grabowski, G., and C. Liu, 2010, Strontium -Isotope age dating and correlation of Phanerozoic anhydrites and un-fossiliferous limestone of Arabia. American Association of Petroleum Geologists, Middle East Geoscience Conference and Exhibition. Manama-Bahrain.
- Jassim, S. Z., and J. C. Goff, 2006, *Geology of Iraq: Dolin*, Prague and Moravian Museum, Brno, Czech Republic, 341p.
- Moor, C. H., 2001, Carbonate reservoirs: porosity evolution and diagenesis in a sequence stratigraphic framework. Amsterdam Elsevier, 137p.
- Nicholas, G., 2001, *Sedimentological and Stratigraphy*. ed. Blackwell Science Ltd, Oxford.
- NOC, 1977, Final well report of well number 10, Ajeel field.
- Rashid, F., P. W. J. Glover, P. Lorinczi, R. Collier, and J. Lawrence, 2015 a, Porosity and permeability of tight carbonate reservoir rocks in the north of Iraq. *Journal of Petroleum Science and Engineering*, v. 133, p. 147-161.
- Rashid, F., P. W. J. Glover, P. Lorinczi, R. Collier, and J. Lawrence 2015 b, Permeability Prediction in Tight Carbonate Rocks Using Capillary Pressure Measurements. *Journal of Marine and Petroleum Geology*, 68A, 536-550.
- Rashid, F., Glover, P.W.J. Lorinczi, P., Hussein, D., and Lawrence, J. (2017) Microstructural controls on reservoir quality in tight oil carbonate reservoir rocks. *Journal of Petroleum Science and Engineering*, 156, 814-826.
- Sayyab, A. S., and A. A. Abid, 1990, Nummulitidae (Foraminifera) from the basal conglomeratic bed at Khan-Al-Baghdadi area, Western Iraq: *Iraq Geol J*, v. 23, p. 46-59.
- Sissakian, V. K., Ibrahim, E. I., Ibrahim, F. A. & Al-Ali, N. M. 2000. Geological map of Iraq, 1/1000000. Baghdad, Iraq. State Company of geological survey and mining.
- Tucker, M. E., V. P. Wright, and J. Dickson, 1990, *Carbonate Sedimentology*. Wiley-Blackwell.
- Wennberg, O. P., T. Svånå, M. Azizzadeh, A. M. M. Aqrabi, P. Brockbank, K. B. Lyslo, and S. Ogilvie, 2006, Fracture intensity vs. mechanical stratigraphy in platform top carbonates: the Aquitanian of the Asmari Formation, Khaviz Anticline, Zagros, SW Iran. *Petroleum Geoscience*, v. 12, p. 235-246.

Western Zagros, 2011, Final well report of well number 1, Kurdamir licence block.

Western Zagros, 2011, Final well report of well number 1, Sarqala licence block.

Zebari, M. M., and C. M. Burberry, 2015, 4-D evolution of anticlines and implications for hydrocarbon exploration within the Zagros Fold-thrust Belt, Kurdistan region, Iraq. *Geo Arabia*, v. 20, p. 161-188.

### **List of Figures**

**Figure 1:** Geological map of Kurdistan region and north east of Iraq shows the selected fields, blocks and outcrop section of the study area, modified from (Sissakian et al., 2000).

**Figure 2:** Chronostratigraphic chart of Iraq (after Petroleum Geo-service, 2000).

**Figure 3:** A Latest Chattian-Early Aquitanian palaeogeography of Iraq, B Late Aquitanian- early Burdigalian palaeogeography of Iraq (after Aqrabi et al., 2010).

**Figure 4:** A-Field photograph of reefal limestone of the Oligocene Anah Formations in the Darzila sections, B-Field photograph of the limestone conglomeratic beneath of the Euphrates Formation in the Awa Spi section, C-Field photograph of the palaeosols layer in the Darzila section.

**Figure 5:** Stratigraphic sections of the Lower Miocene Formations along surface sections, showing thickness, lithological variations and the identified microfacies of the Euphrates Formation (E1, E2, E3, E4 and E5) also with the Jeribe microfacies (J1, J2, J3, J4, J5 and J6). Refer to Figure 1 for outcrop locations

**Figure 6:** Stratigraphic sections of the Lower Miocene Formations along an approximately east to west transect, indicating gross lithological and thickness variations.

**Figure 7:** A Field photograph of the “brecciated”, highly jointed basal layer of the Euphrates Formation from the Darzila outcrop section. B Photomicrograph of the “brecciate” basal unit of the Euphrates Formation: a - reworked fossil from underlying beds, b - intraclast, c - angular quartz grain. Stained thin section from the Awa Spi outcrop section.

**Figure 8:** Field photograph of the evaporitic carbonate of the Jeribe Formation from Mamlaha section.

**Figure 9:** A- Photomicrograph of the brecciated grainstone B1 microfacies. Stained thin section from the Darzila outcrop section.

B- Photomicrograph of the bioclastic-Miliolid grainstone microfacies E1: a - miliolids, b - shell fragment, c - Rotaliids. Stained thin section from the Awa Spi outcrop section, stained thin section from the Darzila section.

C- Photomicrograph of the peloidal grainstone microfacies E2: a - ooids filled by ferroan calcite cement (arrowed) in a stained thin section from the Mamlaha outcrop section.

D- Photomicrograph of ooidal grainstone microfacies E3: a - rounded ooids, b - ellipsoid ooid. Stained thin section from the Awa Spi outcrop section.

E- Photomicrograph of the bioclastic ooidal grainstone microfacies E4.

F- Photomicrograph of the mudstone microfacies E5, mainly composed of lime mud. Stained thin section from the Awa Spi outcrop section.

**Figure 10:** A- Photomicrograph of the quartz-mudstone microfacies J1, with silt size angular quartz grains.

B- Photomicrograph of quartz-wackestone microfacies J2, with cemented molds after bioclastic grains. Stained thin section from the Awa Spi outcrop section.

C- Photomicrograph of bioclastic-packstone microfacies J3. Stained thin section from the well HR2.

D- Photomicrograph of gastropod-grainstone microfacies J4. Stained thin section from the Darzila outcrop section.

E- Photomicrograph of the evaporitic-carbonate microfacies J5. Stained thin section from the Mamlaha outcrop section.

F- Photomicrograph of the miliolids-packstone microfacies J6. Stained thin section from the Darzila section.

**Figure 11:** Depositional model for the Lower Miocene carbonate ramp of the Euphrates and Jeribe Formations in the Kurdistan region, NE Iraq.

### **List of Tables**

Table 1: Geographic locations and samples types at studied surface sections.

Table 2: Geographic locations and well data at studied wells.

Table 3: Summary of microfacies, their main components and interpreted depositional environments for the Euphrates Formation. Gst. (grainstone), Pst. (packstone), Wst. (wackestone), Mst. (mudstone).

Table 4: Summary of microfacies, their main components and interpreted depositional environments of the Jeribe Formation. Gst. (grainstone), Pst. (packstone), Wst. (wackestone), Mst. (mudstone).